Biochem. J. (1991) 278, 721–727 (Printed in Great Britain)

Glucosidase II from rat liver microsomes

Kinetic model for binding and hydrolysis

Josefa Maria ALONSO, Angelines SANTA-CECILIA and Pedro CALVO*
Departamento de Bioquímica y Biología Molecular, Universidad de León, 24007 León, Spain

Glucosidase II is an enzyme involved in glycoprotein biosynthesis, releasing both α-1,3-linked glucose residues from the protein-linked oligosaccharide $Glc_2Man_9GlcNAc_2$-R in the processing of *N*-glycans. We studied the kinetic properties of the enzyme, purified to homogeneity and, for the first time, we have been able to demonstrate the occurrence of two active sites in this enzyme and to establish the mechanisms of binding and hydrolysis of the physiological substrate at its active site(s). The analyses of data fitting to single and double hyperbolic equations and the Eadie–Hofstee profile, together with the inhibition kinetics, demonstrate that the enzyme has two different active sites. The K_m and $V_{max.}$ values for the high-affinity site (site 1) were 0.78 mM and 437 munits/mg respectively, whereas the values for the low-affinity site (site 2) were 481 mM and 13797 munits/mg respectively, for the *p*-nitrophenyl α-D-glucopyranoside substrate. The $V_{max.}/K_m$ ratios, which indicate the efficacy of an active site for a substrate, were 560 and 28.7 ml/min per g for active sites 1 and 2, respectively. The inhibition type, with respect to site 1, for glucose, maltose, D-glucone-δ-lactone, $CaCl_2$ and $MgCl_2$ was pure-competitive, partial-competitive, parabolic, non-competitive and non-competitive respectively. K_i values for glucose, maltose, $CaCl_2$ and $MgCl_2$ were 6.75, 2.05, 10.60 and 14.20 mM respectively. Thus glucose would bind to active site 1, maltose to site 2 (and near to site 1) and D-glucone-δ-lactone to either site 1 or 2. The following hydrolysis mechanism for the physiological substrate ($Glc_2Man_9GlcNAc_2$-protein) of glucosidase II may be concluded from all the foregoing kinetic evidence: the external glucose would be the first released residue, at active site 2, thereafter producing $Glc_1Man_9GlcNAc_2$-protein; the remaining glucose would be released at active site 1, delivering the $Man_9GlcNAc_2$-protein product, which would leave the enzyme.

INTRODUCTION

N-Glycans of glycoproteins are not biosynthesized directly in their definitive form; they pass through intermediate states. The first step in the biosynthesis of the *N*-glycosyl fraction is the block transfer of the oligosaccharide $Glc_3Man_9GlcNAc_2$, conjugated with dolichyl diphosphate, to target asparagine residues of the nascent protein acceptor. In the steps that follow, the oligosaccharides of the newly formed glycoprotein are further trimmed. The trimming sequence is initiated by removal of the three glucose residues. There are two different glucosidases responsible for trimming the oligosaccharide. Glucosidase I activity releases the terminal α-1,2-linked glucose, whereas glucosidase II activity releases the remaining inner two α-1,3-linked glucose residues. These two enzymes are located in microsomal membranes [1,2]. Both glucosidase II and *p*-nitrophenyl-α-D-glucosidase activities are catalysed by the same neutral glucohydrolase [2–4]. Glucosidase I does not show any measurable activity toward this artificial substrate [5], strongly supporting the notion that glucosidase II activity can be assayed as *p*-nitrophenyl-α-D-glucosidase activity in microsomal membranes.

The purification and preliminary studies on the physicochemical properties of glucosidase II from rat liver microsomes have been previously carried out by us [6].

In the present paper we studied its kinetic properties and, for the first time, we demonstrate the occurrence of two active sites in this enzyme and establish the mechanism of binding and hydrolysis of the physiological substrate at its active site(s).

MATERIALS AND METHODS

Materials

p-Nitrophenyl glycosides and D-glucone-δ-lactone were obtained from Sigma Chemical Co., St. Louis, MO, U.S.A. Hepes and Triton X-100 were from Boehringer-Mannheim, Mannheim, Germany. Tris base, 2-mercaptoethanol, D-glucose, maltose and other chemicals, of the highest commercial purity, were from Merck, Darmstadt, Germany.

Animals

After weaning, 28-day-old Wistar rats weighing about 100 g were kept at a constant temperature (20–22 °C) on a 12 h light/dark cycle, fed A-04 rat chow from Panlab (Barcelona, Spain) containing 17% (w/w) protein, 3% (w/w) lipids and 59% (w/w) carbohydrate, and had free access to water. Male rats weighing 300–400 g were used.

Enzyme assay

Glucosidase II activity was assayed at 37 °C in 1 ml of reaction mixture containing 50 mM-Hepes buffer, pH 6.8, 1% sodium cholate and different concentrations of *p*-nitrophenyl α-D-glucopyranoside (pNP-Glc). After incubation, the reaction was stopped with 1 ml of 0.5 M-Na_2CO_3 and the *p*-nitrophenol released was estimated spectrophotometrically at 400 nm. A unit of enzyme activity was defined as the amount of enzyme that catalyses the release of 1 μmol of *p*-nitrophenol/min under

Abbreviations used: Con A, concanavalin A; GlcNAc, *N*-acetylglucosamine; PMSF, phenylmethanesulphonyl fluoride; pNP-Glc, *p*-nitrophenyl α-D-glucopyranoside.

* To whom correspondence should be sent.

optimal conditions. Specific activities are expressed as munits of enzyme/mg of protein.

Protein determination

Protein was determined by a modification of the Lowry procedure [7], with BSA as standard.

Enzyme purification

Male Wistar rats (300–350 g) were killed, without starvation, by decapitation. The livers were minced and washed in 0.25 M-sucrose solution containing 10 mM-Tris/HCl buffer (pH 8.0), 5 mM-2-mercaptoethanol and a proteinase-inhibitor cocktail [1 mM-phenylmethanesulphonyl fluoride (PMSF), 1 mM-1,10-phenanthroline and 1 mM-sodium bisulphite]. Microsomal membranes were prepared as previously described [4]. Glucosidase II from microsomes was purified to electrophoretic homogeneity by solubilization, protamine sulphate precipitation, anion-exchange (DEAE-Sephacel) and affinity [concanavalin A (Con A)-Sepharose-4B] chromatographies [6].

Determination of kinetic parameters

Experimental data were best fitted to a two-active-site model. A modified form of the Michaelis–Menten equation was used for the steady-state kinetics:

$$v = [V_{max.,1}[S]/(K_{m,1}+[S])] + [V_{max.,2}[S]/(K_{m,2}+[S])]$$

where 1 and 2 correspond to the above two active sites. Kinetic parameters were determined by the non-linear regression data-analysis programs ENZFITTER (Elsevier Biosoft) and PCNONLIN (Statistical Consultants) for IBM-PC computers and compatible systems.

Kinetic data were also represented by Eadie–Hofstee plot, and the equation used for curve fitting was a two-site model, adapted from that corresponding to the Scatchard plot described by Rodbard & Feldman [8], which assumes the presence of two distinct independent sites:

$$y = \tfrac{1}{2}(V_{max.,1}+V_{max.,2}-x(K_{m,1}+K_{m,2})+\sqrt{\{[x(K_{m,1}+K_{m,2}) - V_{max.,1}-V_{max.,2}]^2-4x^2K_{m,1}K_{m,2}+4x(V_{max.,1}K_{m,2}+V_{max.,2}K_{m,1})\}})$$

where $y = v$ and $x = v/[S]$.

The inhibition type was determined from double-reciprocal and Dixon plots, with glucose, maltose, D-glucono-δ-lactone, $CaCl_2$ and $MgCl_2$ as inhibitors. Inhibitor constants (K_i) were determined by Dixon plots, and replots of data from double-reciprocal plots. When replots and Dixon plots were not linear, the K_i value was obtained from secondary replots (see below).

RESULTS

Occurrence of two active sites for the hydrolysis of *p*-nitrophenyl α-D-glucopyranoside (pNP-Glc) in glucosidase II from rat liver

By using the purified enzyme (a single band on PAGE) and a broad concentration range (0.08–14 mM) for the substrate pNP-Glc, the saturation phase cannot be approached by plotting v against [pNP-Glc] (Fig. 1*a*). Additionally, the data were well fitted to a two-active-site model by Eadie–Hofstee plot (v against v/[pNP-Glc]; Fig. 1*b*) (see the Materials and methods section), which results in a curved profile. Moreover, the data were not well fitted to a single hyperbolic equation by non-linear regression, as confirmed by the analysis of residuals (Fig. 1*c*, inset). By contrast, they were perfectly fitted to a double-hyperbolic equation (Fig. 1*a*).

All the above-mentioned results indicate that this enzyme has two active sites for the substrate. This finding is confirmed by the rest of the kinetic evidence.

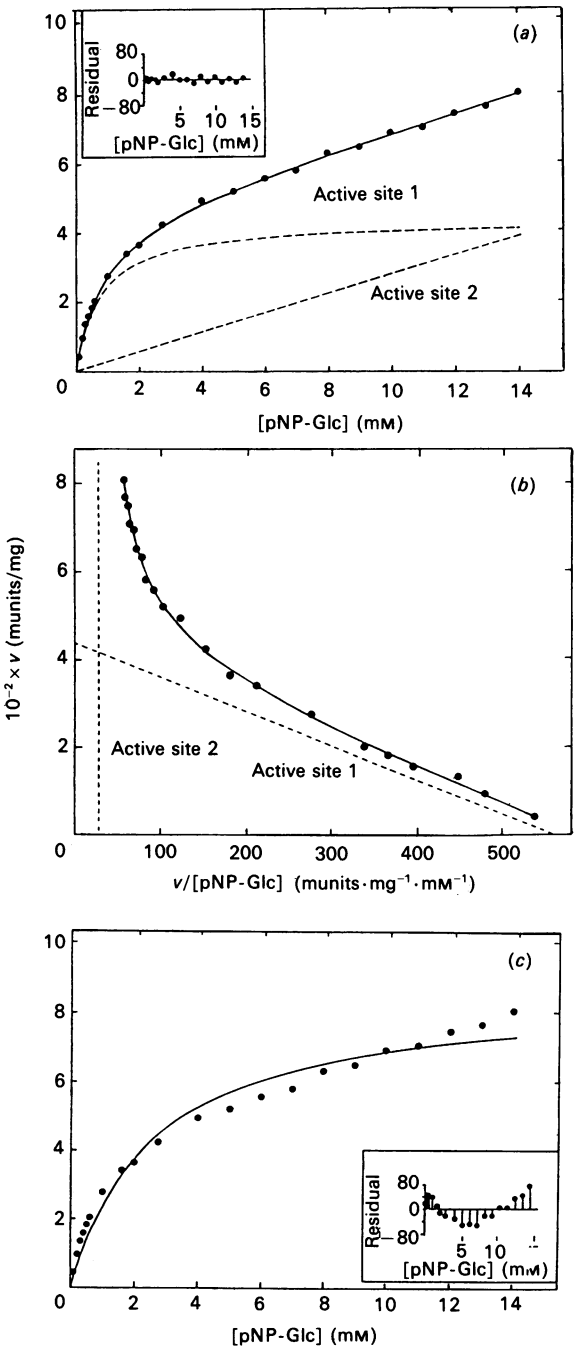

Fig. 1. Occurrence of two active sites in glucosidase II from rat liver

(*a*) Fitting of direct plot to a double-hyperbolic equation. The inset shows residuals plotted versus [pNP-Glc]. (*b*) Eadie–Hofstee plot adapted for two active sites. The theoretical plots corresponding to each active site are indicated by broken lines in (*a*) and (*b*). (*c*) Fitting of the direct plot to a single hyperbolic equation. The inset shows residuals plotted versus [pNP-Glc]. pNP-α-D-glucosidase activity was assayed as indicated in the Materials and methods section.

Similar values were obtained for kinetic parameters using both the Michaelis–Menten and the Eadie–Hofstee equations, adapted to the two-active-site models indicated in the Materials and methods section.

K_m and $V_{max.}$ values for the high-affinity site (site 1) were 0.78 mM and 437 munits/mg respectively (Table 1), whereas these values for the low-affinity site (site 2) were 481 mM and 13797 munits/mg respectively (Table 1), for the substrate pNP-

Table 1. Kinetic parameters of the two active sites of glucosidase II

Enzyme activity was assayed under the conditions described in the Materials and methods section. pNP-Glc was used as substrate at concentrations ranging from 0.06 to 14 mM. K_m and $V_{max.}$ values are means ± S.E.M.

Active site	K_m^* (mM)	$V_{max.}^*$ (munits/mg)	$V_{max.}/K_m$ (ml/min per g)
1 (High affinity)	0.780 ± 0.004	437 ± 1.1	560
2 (Low affinity)	481 ± 15.7	13797 ± 441	28.7

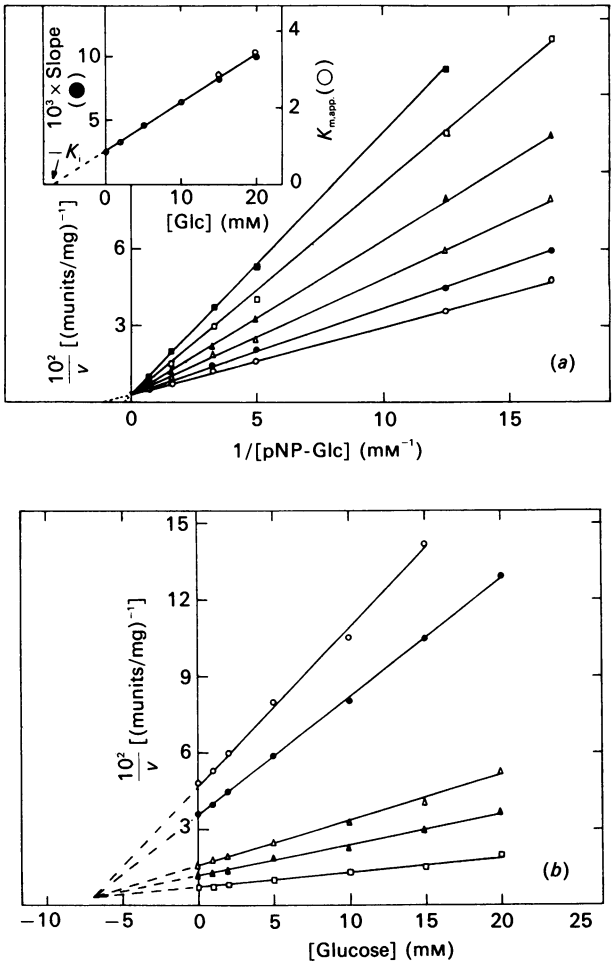

Fig. 2. Inhibition by glucose of pNP-α-D-glucosidase activity of glucosidase II from rat liver

(*a*) Reciprocal plots. Glucose concentrations were: ○, 0; ●, 2 mM; △, 5 mM; ▲, 10 mM; □, 15 mM; ■, 20 mM. The inset shows replots of $K_{m,app.}$ (○) and slope (●) against [glucose]. (*b*) Dixon plots. pNP-Glc concentrations were: ○, 0.06 mM; ●, 0.08 mM; △, 0.20 mM; ▲, 0.30 mM; □, 0.60 mM. pNP-α-D-glucosidase activity was assayed as indicated in the Materials and methods section.

Glc. It should be considered that the latter values (for active site 2) are subject to a higher degree of error, since the maximum substrate concentration that can be obtained under these experimental conditions is about 15 mM, owing to the low substrate solubility. The low level of occupancy of low-affinity sites precludes more accurate measurement of its kinetic parameters.

The $V_{max.}/K_m$ ratios, which indicate the efficacy of an active site for a substrate [9], were 560 and 28.7 ml/min per g for active sites 1 and 2 respectively (Table 1).

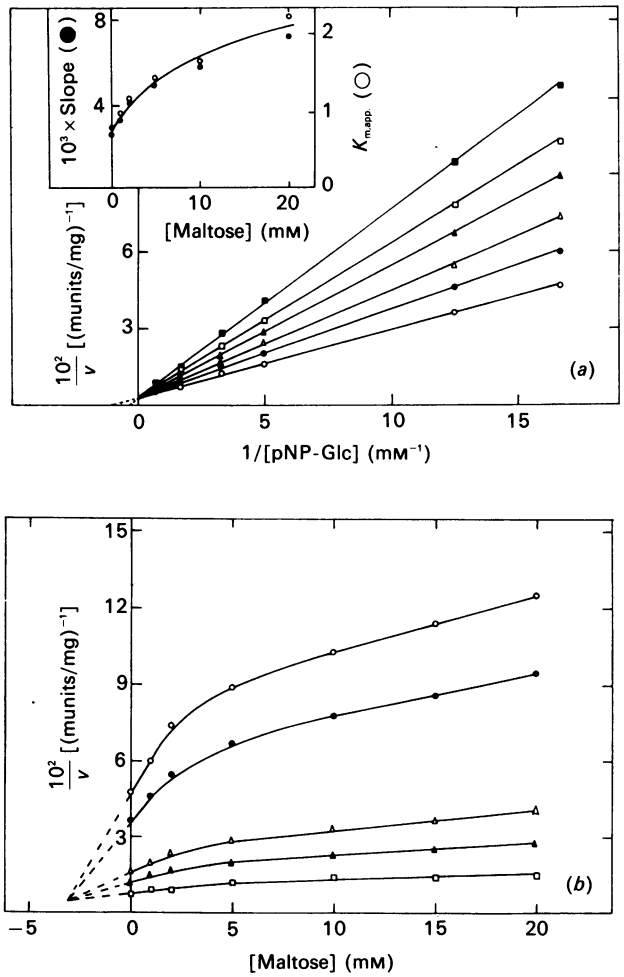

Fig. 3. Inhibition by maltose of pNP-α-D-glucosidase activity of glucosidase II from rat liver

(*a*) Reciprocal plots. Maltose concentrations were: ○, 0; ●, 1 mM; △, 2 mM; ▲, 5 mM; □, 10 mM; ■, 20 mM. The inset shows replots of $K_{m,app.}$ (○) and slope (●) against [maltose]. (*b*) Dixon plots. pNP-Glc concentrations were: ○, 0.06 mM; ●, 0.08 mM; △, 0.20 mM; ▲, 0.30 mM; □, 0.60 mM. pNP-α-D-glucosidase activity was assayed as indicated in the Materials and methods section.

Table 2. Inhibition study of glucosidase II

Enzyme activity was assayed under the conditions described in the Materials and methods section. pNP-Glc was used as substrate at concentrations ranging from 0.06 to 1.6 mM. K_i values are means ± S.E.M.

Inhibitor	[Inhibitor] (mM)	Inhibition type	K_i (mM)
Glucose	1–20	Competitive	6.75 ± 0.32
Maltose	1–20	Partial-competitive	2.05 ± 0.09
D-Glucono-δ-lactone	2–15	Parabolic	–
$CaCl_2$	2–10	Non-competitive	10.6 ± 0.68
$MgCl_2$	2–20	Non-competitive	14.20 ± 0.97

Inhibition analysis for glucose, maltose and D-glucono-δ-lactone

The inhibition analysis for glucose, maltose and D-glucono-δ-lactone was carried out at substrate (pNP-Glc) concentrations ranging between 0.06 and 1.6 mM, involving mainly active site 1.

A typical double-reciprocal analysis of the inhibiting effect of

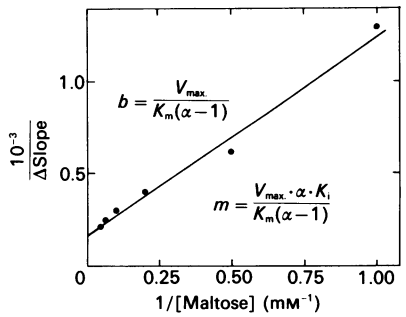

Fig. 4. Secondary replot of 1/(Δ slope) of Fig. 3(*a*) against 1/[maltose] for the determination of K_i

m is the slope; *b* is the intersect.

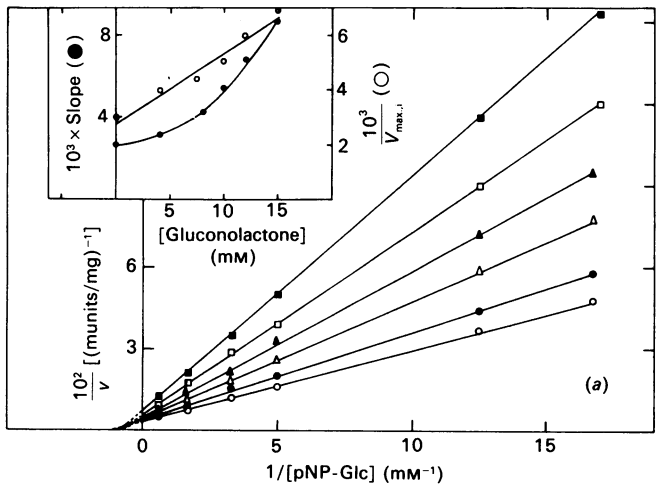

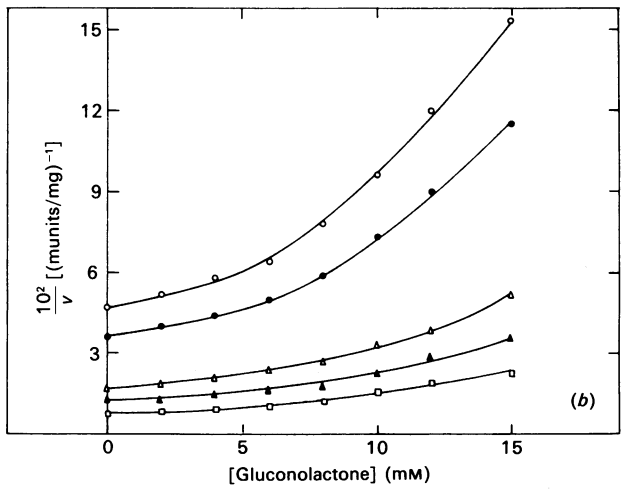

Fig. 5. Inhibition of pNP-α-D-glucosidase activity of glucosidase II from rat liver, by D-glucono-δ-lactone

(*a*) Reciprocal plots. D-Glucono-δ-lactone concentrations were: ○, 0 mM; ●, 4 mM; △, 8 mM; ▲, 10 mM; □, 12 mM; ■, 15 mM. The inset shows replots of $V_{max.,i}^{-1}$ (○) and slope (●) against [lactone]. (*b*) Dixon plots. pNP-Glc concentrations were: ○, 0.06 mM; ●, 0.08 mM; △, 0.20 mM; ▲, 0.30 mM; □, 0.60 mM. pNP-α-D-glucosidase activity was assayed as indicated in the text.

glucose on enzyme activity is shown in Fig. 2(*a*). It is clear that glucose acts as a competitive inhibitor for the pNP-α-D-glucosidase activity of glucosidase II. Dixon plots resulted in straight lines (Fig. 2*b*) intersecting at a common point in the upper-left

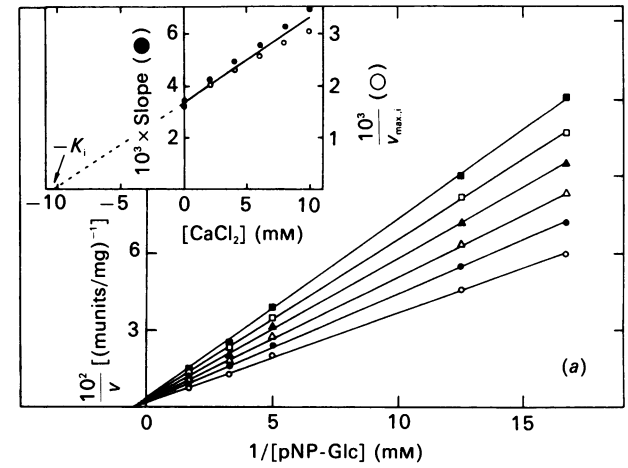

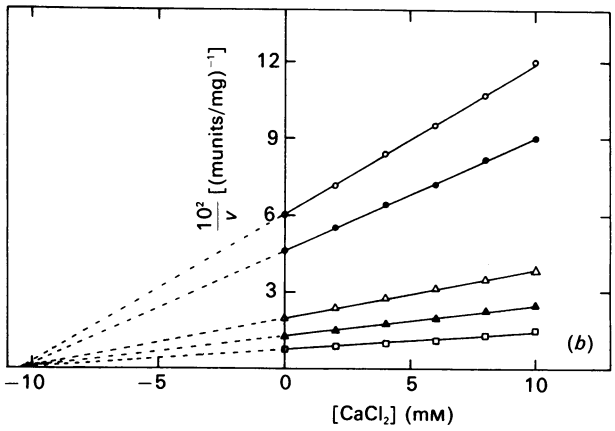

Fig. 6. Inhibition by $CaCl_2$ of pNP-α-D-glucosidase activity of glucosidase II from rat liver

(*a*) Reciprocal plots. $CaCl_2$ concentrations were: ○, 0; ●, 2 mM; △, 4 mM; ▲, 6 mM; □, 8 mM; ■, 10 mM. The inset shows replots of the $V_{max.,i}^{-1}$ (○) and slope (●) against [$CaCl_2$]. (*b*) Dixon plots. pNP-Glc concentrations were: ○, 0.06 mM; ●, 0.08 mM; △, 0.20 mM; ▲, 0.30 mM; □, 0.60 mM. pNP-α-D-glucosidase activity was assayed as indicated in the text.

quadrant. This profile confirms the competitive type of inhibition. When the intersecting point was projected on the horizontal axis, a K_i value of 6.75±0.32 mM was obtained (Table 2). A similar value was determined from replots of slope and $K_{m,app.}$ obtained from double-reciprocal plots, against glucose concentration (Fig. 2*a*, inset).

The fact that replots and Dixon plots give straight lines indicates that the inhibition type for glucose is purely competitive with respect to active site 1.

Maltose also inhibited the enzyme's activity by competition with pNP-Glc (Fig. 3*a*). Replots of slope and $K_{m,app.}$, obtained from double-reciprocal plots, against maltose concentration (Fig. 3*a*, inset), and Dixon plots (Fig. 3*b*), are not linear, but convex-upward, indicating that maltose acts as a partial-competitive inhibitor [10] with respect to active site 1.

A K_i value of 2.05±0.09 mM (Table 2) was obtained from the secondary replots of 1/Δ slope of double-reciprocal plots against 1/[maltose], as described by Segel [11] (Fig. 4). With α (4.3; see Scheme 1 in the Discussion) determined from the intercept (*b*), K_m and $V_{max.}$ from the control ([I] = 0) plot, K_i was calculated from the slope (*m*), as indicated in the Figure.

Using D-glucono-δ-lactone as an inhibitor, in double-reciprocal plots a family of straight lines converging in the upper-left

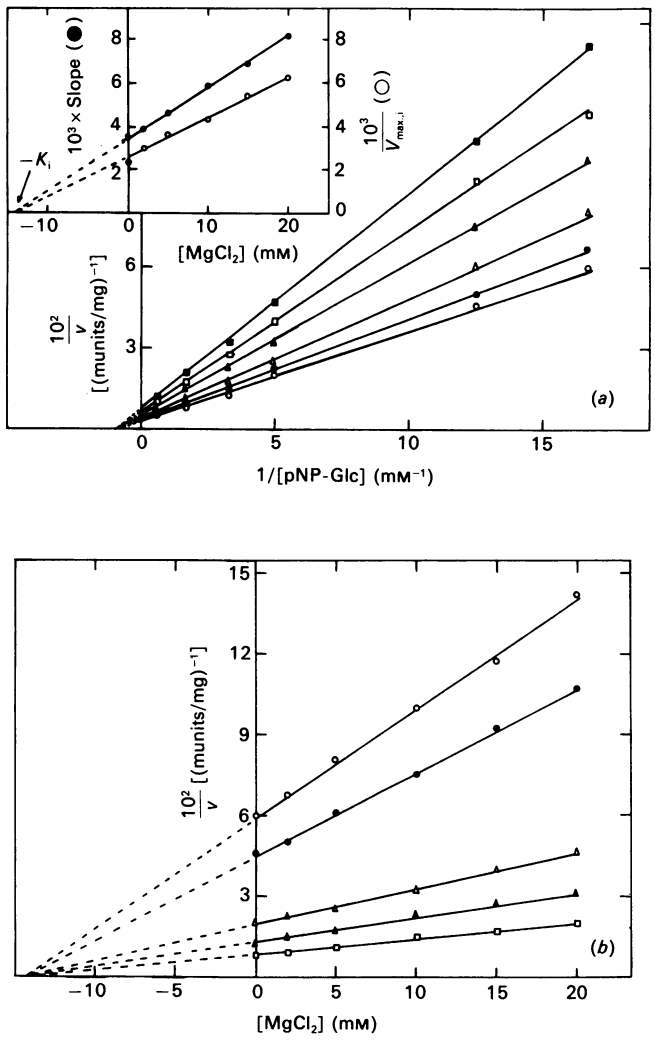

Fig. 7. Inhibition by $MgCl_2$ of pNP-α-D-glucosidase activity of glucosidase II from rat liver

(*a*) Reciprocal plots. $MgCl_2$ concentrations were: ○, 0; ●, 2 mM; △, 5 mM; ▲, 10 mM; □, 15 mM; ■, 20 mM. The inset shows replots of $V_{max.,i}^{-1}$ (○) and slope (●) against [$MgCl_2$]. (*b*) Dixon plots. pNP-Glc concentrations were: ○, 0.06 mM; ●, 0.08 mM; △, 0.20 mM; ▲, 0.30 mM; □, 0.60 mM. pNP-α-D-glucosidase activity was assayed as indicated in the text.

quadrant (Fig. 5*a*) but non-intersecting at a common point is obtained. The profiles of the replot of intercepts of double-reciprocal plots against lactone concentration (Fig. 5*a*, inset) are linear, whereas the replot of slope of double-reciprocal plots against lactone concentration (Fig. 5*a*, inset) and the Dixon plots (Fig. 5*b*) are not linear, but parabolic, indicating that D-glucono-δ-lactone acts as a parabolic inhibitor [12], as will be discussed below.

Inhibition analysis for $CaCl_2$ and $MgCl_2$

The profiles of the double-reciprocal plots (Fig. 6*a*), the replots of slope and intercept, obtained from double-reciprocal plots, against $CaCl_2$ concentration (Fig. 6*a*, inset), together with the Dixon plots (Fig. 6*b*) correspond to non-competitive inhibition for $CaCl_2$. The K_i value (10.6±0.68 mM) obtained from the replots (Table 2) was similar to that obtained from Dixon plots.

Fig. 7(*a*) shows a family of straight lines intersecting at a common point on the horizontal axis, obtained by means of double-reciprocal plots at different $MgCl_2$ concentrations. Furthermore, the Dixon plots (Fig. 7*b*) intersect at a common point on the horizontal axis. Therefore $MgCl_2$ acts as a non-competitive inhibitor of pNP-α-D-glucosidase activity of glucosidase II. The K_i value obtained from replots (Fig. 7*a*, inset) and Dixon plots (Fig. 7*b*) was 14.20±0.97 mM.

DISCUSSION

This enzyme shows kinetic evidence for a two-active-site model. Negative co-operativity of the presence of multiple enzymes could also exhibit similar kinetic profiles. Nevertheless, the whole kinetic model and the homogeneity of our enzyme preparation (a single band by PAGE) preclude these later hypothesis. Additionally, there is no report about co-operativity for this or related enzymes.

The $V_{max.}/K_m$ ratios (Table 1) indicate that active site 1 is 20 times more efficient than site 2 for the substrate used. From the K_m values it can be concluded that site 1 has 617 times more affinity than site 2 for this substrate. Therefore, using this synthetic substrate, active site 1 is the site mainly responsible for catalytic activity at low and normal substrate concentrations (Fig. 1*a*).

In inhibition studies, the substrate pNP-Glc binds almost exclusively to active site 1 at the concentrations used (0.06–1.6 mM).

Glucose behaves as a pure competitive inhibitor (Figs. 2*a* and 2*b*), competing with pNP-Glc in active site 1 (Scheme 3*a* below).

Maltose acts as a partial-competitive inhibitor for the pNP-α-glucosidase activity of glucosidase II (Figs. 3*a* and 3*b*). The equilibria describing this situation are shown in the following Scheme [10]:

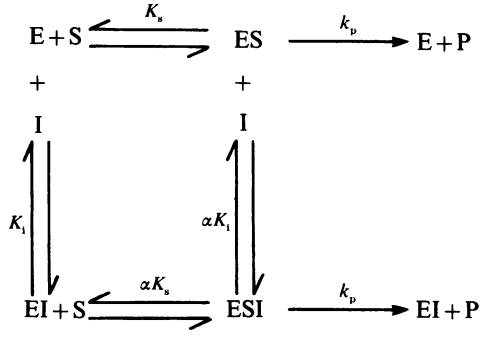

Scheme 1.

The substrate (pNP-Glc) and maltose would bind to the enzyme (E) at different sites to yield E–pNP-Glc, E–maltose, and maltose–E–pNP-Glc complexes. E–pNP-Glc and maltose–E–pNP-Glc yield products with equal facility, and the velocity of the reaction can never be driven to zero because at infinitely high maltose concentrations pNP-Glc can always bind to the site unoccupied by maltose, to be hydrolysed there. The K_m value will increase because at any maltose concentration a portion of the available enzyme exists in the form E–maltose, having a decreased affinity for pNP-Glc ($\alpha K_s > K_s$, $\alpha = 4.3$ in our case).

In our model maltose would bind to the enzyme on active site 2, by one of its glucose moieties. The other glucose moiety of the disaccharide would be located close to site 1, hindering, but not excluding, the binding of the substrate (pNP-Glc) to this site (Scheme 3*b* below).

D-Glucono-δ-lactone acts as a parabolic inhibitor (Figs. 5*a* and 5*b*). The profiles of the slope replot and Dixon plots are parabolas, indicating that the lactone would bind to the enzyme at two different, but not mutually exclusive, sites. Therefore an EI_2 complex could be formed. In this case, as proposed by Segel [12], the reciprocal-plot patterns are essentially unchanged (Fig. 5*a*),

although the plots do not now all intersect at a common point (in the upper-left quadrant). The scheme would be as follows:

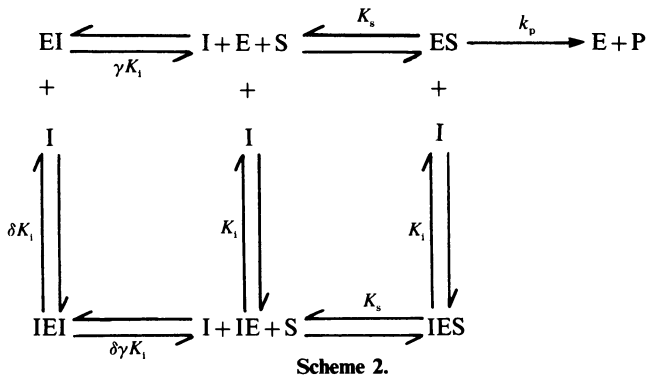

Scheme 2.

In this inhibition type, the binding of the inhibitor to one of the inhibitor sites (active site 1 in our model) excludes the binding of the substrate (pNP-Glc), but the binding of the inhibitor to the other inhibitor site (site 2 in our model) has no effect on the binding of the substrate; however, the resulting IES (lactone–E–pNP-Glc) complex is catalytically inactive. Scheme 3(*c*) shows the different complexes for our model.

The velocity equation is:

$$\frac{v}{V_{max.}} = \frac{[S]}{K_s\left(1+\frac{[I]}{K_i}+\frac{[I]}{\gamma K_i}+\frac{[I]^2}{\delta\gamma K_i^2}\right)+[S]\left(1+\frac{[I]}{K_i}\right)}$$

The slope and intercept for reciprocal plots are:

$$\text{Slope} = \frac{K_s}{V_{max.}}\left(1+\frac{[I]}{K_i}+\frac{[I]}{\gamma K_i}+\frac{[I]^2}{\delta\gamma K_i^2}\right)$$

$$\text{Intercept} = \frac{1}{V_{max.}}\left(1+\frac{[I]}{K_i}\right)$$

Therefore, the slope and the intercept are parabolic and linear functions of [I] respectively. This fact explains why the family of straight lines does not intersect at a common point in reciprocal plots (Fig. 5*a*).

Maltose behaves as a stronger inhibitor (lower K_i value, Table 2) for pNP-α-glucosidase activity of glucosidase II than glucose, which is consistent with the proposed model, since maltose is more similar to the physiological substrate (in its binding part) than glucose.

D-Glucone-δ-lactone is a stronger inhibitor than glucose, which probably makes possible its binding to active site 2 (in addition to 1), because of its half-chair configuration, similar to that of the transition state of the enzyme reaction.

The results for inhibition type obtained with maltose and D-glucone-δ-lactone are in agreement with the occurrence of two binding sites for pNP-Glc, as proposed by non-linear-regression fitting to a double-hyperbolic equation (Fig. 1*a*) and by the Eadie–Hofstee plot (Fig. 1*b*).

Datema *et al.* [13] have suggested that the active site of glucosidase II may contain two glucose-binding sites in order to explain why bromoconduritol, a covalent inhibitor of α-glucosidases, inhibits the trimming of only the innermost glucose residue of the oligosaccharide $Glc_3Man_9GlcNAc_2$.

All the above-mentioned kinetic evidence supports the model for the binding and hydrolysis of the physiological substrate ($Glc_2Man_9GlcNAc_2$-protein) of glucosidase II, presented in Scheme 3(*d*). Since the oligosaccharide intermediate $Glc_1Man_9GlcNAc_2$ has been detected in the processing of the initial substrate [14], the external glucose residue would be the first one released, at active site 2, to produce $Glc_1Man_9GlcNAc_2$-protein. The remaining glucose residue would be released at active site 1, delivering the product $Man_9GlcNAc_2$-protein, which would leave the enzyme.

The pNP-α-glucosidase activity of glucosidase II was non-competitively inhibited by Ca^{2+} and Mg^{2+}, the former being a stronger inhibitor (lower K_i value; Table 2). Burns & Touster [2] reported that Ca^{2+} and Mg^{2+}, at concentrations ranging between 10 and 50 mM, do not affect the cleavage of pNP-Glc by glucosidase II. The differences found in the action of Ca^{2+} and Mg^{2+} on enzyme activity could be explained in terms of the enzyme used by the above-mentioned authors being a product of

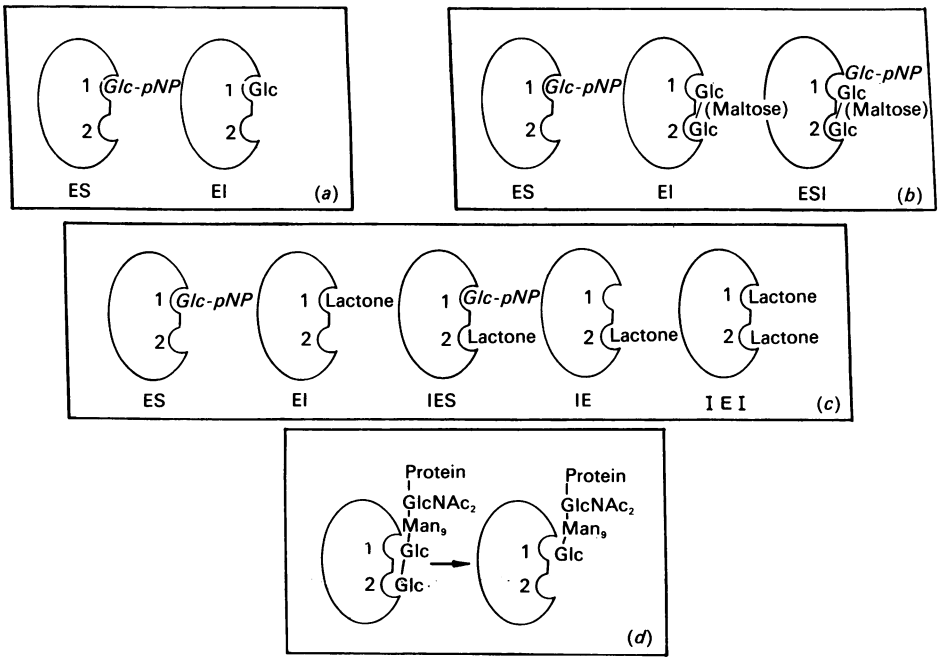

Scheme 3.

partial proteinase degradation, as suggested by Hino & Rothman [4]. On the other hand, the molecular mass of the enzyme purified by us is higher than that reported by Burns & Touster [2] (results not shown). The enzyme integrity and/or the higher purity of our preparation (electrophoretic homogeneity) could explain the different results reported.

This work was supported by a grant from the Fondo de Investigaciones Sanitarias de la Seguridad Social (FISss) (88/0895 and 89/0528), Spanish Ministry of Health.

REFERENCES

1. Grinna, L. S. & Robbins, P. W. (1979) J. Biol. Chem. **254**, 8814–8818
2. Burns, D. M. & Touster, O. (1982) J. Biol. Chem. **257**, 9991–10000
3. Michel, J. M. & Kornfeld, S. (1980) Arch. Biochem. Biophys. **199**, 249–258
4. Hino, Y. & Rothman, J. E. (1985) Biochemistry **24**, 800–805
5. Elting, J. J. & Lennarz, W. J. (1982) Methods Enzymol. **83**, 429–432
6. Santa-Cecilia, A., Alonso, J. M. & Calvo, P. (1991) Biol. Chem. Hoppe-Seyler, in the press
7. Markwell, M. A. K., Haas, S. M., Bieber, L. L. & Tolbert, N. E. (1978) Anal. Biochem. **87**, 206–210
8. Rodbard, D. & Feldman, H. A. (1975) Methods Enzymol. **36**, 3–16
9. Sols, A. & Crane, R. K. (1954) J. Biol. Chem. **210**, 581–595
10. Segel, I. H. (1975) Enzyme Kinetics, pp. 161–165, Wiley–Interscience, New York
11. Segel, I. H. (1975) Enzyme Kinetics, pp. 178–187, Wiley–Interscience, New York
12. Segel, I. H. (1975) Enzyme Kinetics, pp. 176–178, Wiley–Interscience, New York
13. Datema, R., Romero, P. A., Legler, G. & Schwarz, R. T. (1982) Proc. Natl. Acad. Sci. U.S.A. **79**, 6787–6791
14. Kornfeld, S., Li, E. & Tabas, I. (1978) J. Biol. Chem. **253**, 7771–7778

Received 17 December 1990/21 March 1991; accepted 24 March 1991